Mechanistic Pathways for Oxidative Addition of Aryl Halides to Palladium(0) Complexes: A DFT Study

Lukas J. Goossen,*,† Debasis Koley, Holger L. Hermann, and Walter Thiel*

Max-Planck-Institut für Kohlenforschung, D-45470 Mülheim an der Ruhr, Germany

Received January 12, 2005

Density functional calculations on the title reaction are reported using the gradient-corrected BP86 functional with a standard basis (LANL2DZ) and a larger basis of triple-ζ quality (EXT). Several reaction pathways for oxidative addition of aryl halides to Pd(0) species have been explored, particularly for the reaction of phenyl iodide with $Pd(PMe_3)_2OAc^-$. We confirm that three-coordinate anionic Pd(0) species as proposed by Amatore and Jutand are stable intermediates and can serve as starting points for catalytic reactions. However, we did not find any evidence for the existence of the proposed five-coordinate Pd(II) complexes. Instead, stable four-coordinate intermediates were found, in which the aryl halides coordinate linearly to the palladium via the halide atom, with no significant energy barrier. With these adducts as a starting point, two energetically feasible pathways for the actual C−I cleavage reactions have been identified, which both lead to cis-configured Pd(II) complexes. The subsequent cis−trans isomerization requires significantly more activation than all preceding steps during the oxidative addition. The density functional calculations provide a plausible mechanism for the title reaction that is consistent with the available experimental facts.

Introduction

Palladium-catalyzed cross-coupling reactions such as Suzuki reactions, Heck olefinations, Stille couplings, and Buchwald−Hartwig aminations have become indispensable tools of modern organic synthesis.[1−4] The initiating step of all these transformations is the oxidative addition of aryl halides to palladium(0) complexes. In many cases, it is believed to be rate-determining,[5] so that it is essential to understand its detailed mechanism and the factors which influence its efficiency.

Therefore, this oxidative addition step has been the subject of extensive investigations including experimental studies on model systems,[6] kinetic measurements,[7,8] and quantum-chemical calculations.[9−11] Originally, it was proposed that the catalytically active palladium species are coordinatively unsaturated complexes of the Pd^0L_2 type **1**. According to the classical mechanism depicted in Scheme 1, aryl halides **2** oxidatively add to such species, giving rise to trans-configured complexes **3**, which have been isolated and characterized. Complex **3** acts as the starting point for further steps of the catalytic transformations: in the case of C−C coupling reactions, a transmetalation step follows, leading to structure **5**. Due to the trans geometry of this intermediate, an isomerization to compound **6** is necessary before the product can be liberated via reductive elimination.

Scheme 1. Classical Mechanism for Cross-Coupling Reactions

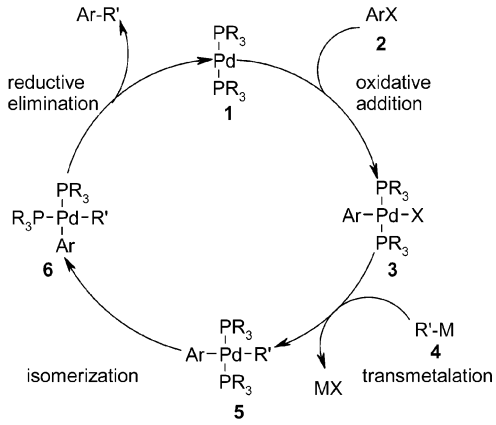

† Current address: Institut für Organische Chemie der RWTH Aachen, Professor Pirlet Str. 1, D-52074, Aachen, Germany. E-mail: goossen@oc.rwth-aachen.de.

(1) (a) Miyaura, N. In *Metal-Catalyzed Cross-Coupling Reactions*, 2nd ed.; Diederich, F., Stang, P. J., Eds.; Wiley-VCH: New York, 2004. (b) Miyaura, N.; Suzuki, A. *Chem. Rev.* **1995**, *95*, 2457.

(2) (a) De Meijere, A.; Meyer, F. E. *Angew. Chem., Int. Ed. Engl.* **1995**, *33*, 2379. (b) Beletskaya, I. P.; Cheprakov, A. V. *Chem. Rev.* **2000**, *100*, 3009.

(3) Stille, J. K. *Angew. Chem., Int. Ed. Engl.* **1986**, *25*, 508.

(4) (a) Wolfe, J. P.; Tomori, H.; Sadighi, J. P.; Yin, J.; Buchwald, S. L. *J. Org. Chem.* **2000**, *65*, 1158. (b) Ehrentraut, A.; Zapf, A.; Beller, M. *Adv. Synth. Catal.* **2002**, *344*, 209 and references therein.

(5) Stille, J. K.; Lau, K. S. Y. *Acc. Chem. Res.* **1977**, *10*, 434.

(6) (a) Roy, A. H.; Hartwig, J. F. *J. Am. Chem. Soc.* **2003**, *125*, 13944. (b) Stambuli, J. P.; Bühl, M.; Hartwig, J. F. *J. Am. Chem. Soc.* **2002**, *124*, 9346.

(7) (a) Casado, A. L.; Espinet, P. *J. Am. Chem. Soc.* **1998**, *120*, 8978. (b) Casado, A. L.; Espinet, P. *Organometallics* **1998**, *17*, 954. (c) Espinet, P.; Echavarren, A. M. *Angew. Chem., Int. Ed.* **2004**, *43*, 4704.

(8) (a) Amatore, C.; Jutand, A. *Acc. Chem. Res.* **2000**, *33*, 314. (b) Amatore, C.; Azzabi, M.; Jutand, A. *J. Am. Chem. Soc.* **1991**, *113*, 1670. (c) Amatore, C.; Jutand, A.; Suarez, A. *J. Am. Chem. Soc.* **1993**, *115*, 9531.

(9) (a) Bickelhaupt, F. M.; Ziegler, T.; Schleyer, P. v. R. *Organometallics* **1995**, *14*, 2288. (b) Diefenbach, A.; Bickelhaupt, F. M. *J. Chem. Phys.* **2001**, *115*, 4030. (c) Albert, K.; Gisdakis, P.; Rösch, N. *Organometallics* **1998**, *17*, 1608. (d) Jakt, M.; Johannissen, L.; Rzepa, H. S.; Widdowson, D. A.; Wilhelm, A. *J. Chem. Soc., Perkin Trans. 2* **2002**, 576.

(10) Sundermann, A.; Uzan, O.; Martin, J. M. L. *Chem. Eur. J.* **2001**, *7*, 1703.

(11) Senn, H. M.; Ziegler, T. *Organometallics* **2004**, *23*, 2980.

10.1021/om0500220 CCC: $30.25
Publication on Web 04/07/2005

Scheme 2. Alternative Pathways for the Oxidative Addition Reaction

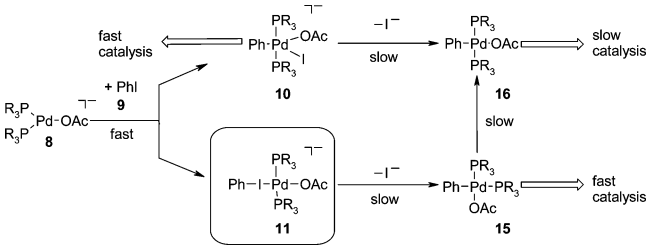

Most of the computational studies are based on this mechanistic concept. A series of calculations were performed by Bickelhaupt et al. to elucidate the elementary steps of the catalytic cycle.[9] They reported on three different types of mechanisms for C−X oxidative addition to a bare d^{10} metal center: a concerted cis oxidative addition of palladium to the C−Cl bond, a backside nucleophilic substitution on the ipso carbon (S_N2 approach), and a radical mechanism via a single-electron transfer (SET).[9] In their calculations, the concerted mechanism for the oxidative insertion via a three-membered transition state was favored. Diefenbach and Bickelhaupt emphasized the quantitative significance of relativistic effects in C−X addition reactions.[9] Sundermann et al. postulated the formation of a η^2-phenyl iodide palladium(0) complex as a starting point for the oxidative addition of the aryl iodide via a nonplanar and perpendicular transition state.[10]

In recent years, the significance of this classical mechanism for palladium-catalyzed reactions has been questioned, since it does not agree with some important experimental findings, especially the pronounced influence that counterions of the palladium(II) precatalysts and added metal salts have on catalytic activities.[8] Furthermore, isolated trans complexes **3** have been found to react only very slowly with organometallic reagents, while catalytic cross-coupling reactions with the same reagents proceed much faster.[7,12] This is expected, since the isomerization from cis to trans should be very slow. Moreover, Espinet et al. observed that the oxidative addition of aryl iodides initially leads to cis complexes, which then isomerize to the more stable intermediate trans complexes **3**.[7]

Amatore and Jutand found that in the reaction of palladium(II) salts with phosphines, three-coordinate anionic palladium(0) complexes **8** are formed instead of the expected two-coordinate complexes **1** (see Scheme 2; substituents R = Me, Ph will be indicated by the appended letters **a** and **b**). The counterion of the precatalyst remains bound to palladium and affects its reactivity. Kinetic studies indicate that upon addition of phenyl iodide **9** to the three-coordinate complex **8b** (R = phenyl), a new species forms quantitatively within seconds, while the solution remains free of iodide and acetate anions. If no further reagent is added, the four-coordinate trans complex **16b** (R = phenyl) is detected several minutes later. To rationalize these findings, Amatore and Jutand proposed a radically different reaction mechanism via three- and five-coordinate palladium species, starting from the five-coordinate structure **10**.[8] However, a dominating role of the five-coordinate palladium species would seem doubtful, as only a few five-coordinate palladium complexes are known which contain constraining polydentate ligands.[13] Furthermore, it is hard to see why the formation of **10**, which requires the cleavage of a strong C−I bond and the formation of two new bonds, should happen within seconds, while the release of an iodide ion to yield the stable trans complex **16** should be so much slower.

Since many experimental findings can be rationalized with the reaction mechanism suggested by Amatore and Jutand, we decided to use it as a starting point for theoretical studies using DFT calculations (BP86/LANL2DZ).[14−17] We first concentrated on the three- and five-coordinate intermediates and could indeed verify the stability of the three-coordinate anionic complexes **8**. However, despite thorough searches, we did not find any evidence for an energy minimum of the five-coordinate anionic complex **10**. Instead, we located a stable minimum for an entirely different structure, **11**, in which the aryl iodide linearly coordinates to palladium via the iodine atom.[18] Furthermore, we were able to show a possible reaction pathway for the oxidative addition of the aryl iodide starting from this intermediate, giving rise to the cis-configured complex **15**. The key findings of our calculations were disclosed in a preliminary communication.[19] Herein we present further theoretical studies on the structure and stability of the key intermediates and discuss alternative pathways for the oxidative addition of aryl halides to anionic palladium(0) species.

Computational Details

All calculations were performed with the Gaussian98 and Gaussian03 program packages.[14] The density functional calculations (DFT) with the BP86 functional[15] employed a basis set of double-ζ quality, which is denoted LANL2DZ in Gaussian. For the heavy elements (e.g. Pd, P, and I) effective core potentials (ECPs)[16] with the corresponding basis set were used, while the light elements (C, H, O) were described by a Dunning/Huzinaga full double-ζ basis set.[17] Geometries were fully optimized, normally without symmetry constraints.

(12) (a) Fauvarque, J. F.; Jutand, A. *J. Organomet. Chem.* **1977**, *132*, C17. (b) Fauvarque, J. F.; Jutand, A. *Bull. Soc. Chim. Fr.* **1976**, 765.

(13) (a) Hansson, S.; Norrby, P.-O.; Sjögren, M. P. T.; Åkermark, B.; Cucciolito, M. E.; Giordano, F.; Vitagliano, A. *Organometallics* **1993**, *12*, 4940. (b) Bröring, M.; Brandt, C. D. *Chem. Commun.* **2003**, 2156.

(14) Frisch, M. J.; Trucks, G. W.; Schlegel, H. B.; Scuseria, G. E.; Robb, M. A.; Cheeseman, J. R.; Montgomery, J. A. Jr.; Vreven, T.; Kudin, K. N.; Burant, J. C.; Millam, J. M.; Iyengar, S. S.; Tomasi, J.; Barone, V.; Mennucci, B.; Cossi, M.; Scalmani, G.; Rega, N.; Petersson, G. A.; Nakatsuji, H.; Hada, M.; Ehara, M.; Toyota, K.; Fukuda, R.; Hasegawa, J.; Ishida, M.; Nakajima, T.; Honda, Y.; Kitao, O.; Nakai, H.; Klene, M.; Li, X.; Knox, J. E.; Hratchian, H. P.; Cross, J. B.; Adamo, C.; Jaramillo, J.; Gomperts, R.; Stratmann, R. E.; Yazyev, O.; Austin, A. J.; Cammi, R.; Pomelli, C.; Ochterski, J. W.; Ayala, P. Y.; Morokuma, K.; Voth, G. A.; Salvador, P.; Dannenberg, J. J.; Zakrzewski, V. G.; Dapprich, S.; Daniels, A. D.; Strain, M. C.; Farkas, O.; Malick, D. K.; Rabuck, A. D.; Raghavachari, K.; Foresman, J. B.; Ortiz, J. V.; Cui, Q.; Baboul, A. G.; Clifford, S.; Cioslowski, J.; Stefanov, B. B.; Liu, G.; Liashenko, A.; Piskorz, P.; Komaromi, I.; Martin, R. L.; Fox, D. J.; Keith, T.; Al-Laham, M. A.; Peng, C. Y.; Nanayakkara, A.; Challacombe, M.; Gill, P. M. W.; Johnson, B.; Chen, W.; Wong, M. W.; Gonzalez, C.; Pople, J. A. *Gaussian 03*; Gaussian, Inc., Pittsburgh, PA, 2003.

(15) (a) Becke, A. D. *Phys. Rev. A* **1988**, *38*, 3098. (b) Perdew, J. P. *Phys. Rev. B* **1986**, *33*, 8822.

(16) Dunning, T. H., Jr.; Hay, P. J. In *Modern Theoretical Chemistry*, Schaefer III, H. F., Ed.; Plenum: New York, 1976; Vol. 3, p 1.

(17) Hay, P. J.; Wadt, W. R. *J. Chem. Phys.* **1985**, *82*, 299.

(18) Boche, G.; Schimeczek, M.; Cioslowski, J.; Piskorz, P. *Eur. J. Org. Chem.* **1998**, 1851 and references therein.

(19) Goossen. L. J.; Koley, D.; Hermann, H.; Thiel, W. *Chem. Commun.* **2004**, 2141.

Harmonic force constants were computed at the optimized geometries to characterize the stationary points as minima or saddle points. Zero-point vibrational corrections were determined from the harmonic vibrational frequencies to convert the total energies E_e to ground-state energies E_0. The rigid-rotor harmonic-oscillator approximation was applied for evaluating the thermal and entropic contributions. Transition states were located from a linear transit scan, in which the reaction coordinate was kept fixed at different distances while all other degrees of freedom were optimized. After the linear transit search, the transition states were optimized using the default Berny algorithm implemented in Gaussian98. The nature of transition states **[12a-13a]**‡, **[13a-14a]**‡, and **[14a-15a]**‡ was verified by following the intrinsic reaction coordinates. Single-point solvent calculations were performed on the optimized gas-phase geometries for all the intermediates and transition states involved in the whole process. We employed the CPCM model,[20] which is an implementation of the conductor-like screening solvation model (COSMO)[21] in Gaussian03. THF was used as solvent with the UAKS (united atom topological model) radii scheme for the respective atoms (Pd, H, C, O, P, I). For further validation, single-point calculations were performed at the optimized BP86/LANL2DZ geometries employing larger basis sets: using quasirelativistic pseudopotentials,[22,23] Pd and I were described by (8s7p5d)/[6s5p3d][22] and SDB-cc-pVTZ[24] valence basis sets, respectively, the aug-cc-pVTZ basis[25] was employed for O, P, and C, and the cc-pVDZ[26] basis was used for all H atoms. The relative energies derived from these BP86/EXT single-point calculations (E_{EXT}) are included in the respective tables, together with the corresponding BP86/LANL2DZ results. These tables document the energetics required for various steps, including ΔE_e (change in electronic energy); ΔE_0 (change in electronic plus zero-point energy); ΔH_{298} (change in thermal enthalpies), ΔG_{298} (change in free energies), ΔE_{sov} (change in electronic energy including solvent effects), and ΔE_{EXT} (change in BP86/EXT single-point electronic energy). We find only minor variations in the computed DFT energies upon basis set extension (ΔE_e vs ΔE_{EXT}), in agreement with a recent systematic benchmark study on the oxidative addition of methane to palladium.[27] The charge distribution around the metal center was analyzed using Weinhold's NPA approach.[28] Wiberg bond indices (WBIs) were also calculated to quantify covalent interactions in the complexes.[29] Contour maps were drawn with the Molden program package.[30]

Results and Discussion

A. Catalytically Active Species. To identify the most likely starting point for the oxidative addition step, we calculated the properties of several coordinatively unsaturated palladium(0) phosphine species at the BP86/LANL2DZ level of theory. Initially, PMe_3 was used as the phosphine ligand to reduce the computational effort. Energy minima were found for the d^{10} complex $Pd(PMe_3)_2$ (**1a**), for the anionic, three-coordinate complex $Pd(PMe_3)_2OAc^-$ (**8a**), as proposed by Amatore and Jutand, and for the coordinatively unsaturated anionic complex $Pd(PMe_3)OAc^-$ (**7a**), similar to that observed by Hartwig et al. for sterically crowded phosphines (Scheme 3). The structural information is summarized in Figure 1.

Scheme 3. Comparison of Several Palladium(0) Species (BP86/LANL2DZ, kcal/mol)

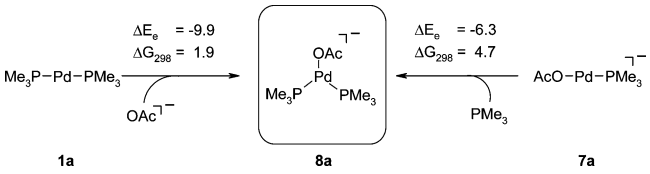

The two phosphines in **1a** are staggered with respect to each other in an essentially collinear P−Pd−P arrangement. The Pd−O bond is shorter in **7a** (2.100 Å) than in **8a** (2.319 Å), indicating a stronger palladium−acetate bond in the former complex.

In **8a**, the palladium is in a distorted-trigonal-planar environment. The P−Pd−P angle amounts to 133.2°, and the two phosphines are staggered with respect to each other. Due to interactions between the carboxylic oxygen of the acetate ligand and hydrogen atoms of one PMe_3 ligand, the acetate lies almost within the PPdP plane, and the two P−Pd−O angles differ by almost 20° (103.7° vs 123.1°). The complexation reactions leading to **8a** (Scheme 3) are computed to be exothermic, by −9.9 kcal/mol from **1a** and −6.3 kcal/mol from $Pd(PMe_3)OAc^-$ (**7a**). They are slightly endergonic at 298 K (by 1.9 and 4.7 kcal/mol, respectively), because of the entropic penalty for gas-phase association reactions.

To get further evidence for the existence of anionic palladium(0) species of the Jutand type, we performed additional calculations on the more realistic $Pd(PPh_3)_2OAc^-$ system **8b** (Figure 2). Geometry optimization at the BP86/LANL2DZ level led to an energy minimum for **8b** with a structure similar to that of **8a**.

The larger steric demand of the PPh_3 ligands in **8b** compared with the PMe_3 ligands in **8a** causes a twisted (P(2)−Pd−O(4)−C = 67.8°) orientation of the acetate ligand relative to the PPdP plane and a larger P−Pd−P angle (136.6° vs 132.2°). The carboxylic oxygen of the acetate interacts only weakly with one of the phenyl hydrogen atoms in **8b**. In comparison with **8a**, the environment of palladium is more symmetrical in **8b** (P−Pd−O angles of 109.2 and 113.5°; Pd−P bond lengths of 2.368 and 2.365 Å). The shorter Pd−O bond (2.304 Å instead of 2.319 Å) suggests that the acetate ligand is more strongly bound in **8b** than in **8a**, and the calculated dissociation energy is indeed significantly higher (21.8 vs 9.9 kcal/mol, BP86/LANL2DZ).

Three-coordinate anionic species were also found with chloride ligands: both $Pd(PMe_3)_2Cl^-$ (**8c**) and $Pd(PPh_3)_2Cl^-$ (**8d**) are energy minima on the BP86/LANL2DZ potential energy surface. Again, **8c** is rather distorted around palladium, while **8d** is more sym-

(20) (a) Barone, V.; Cossi, M. *J. Phys. Chem. A* **1998**, *102*, 1995. (b) Cossi, M.; Rega, N.; Scalmani, G.; Barone, V. *J. Comput. Chem.* **2003**, *24*, 669.
(21) Klamt. A.; Schüürmann, G. *J. Chem. Soc., Perkin Trans. 2* **1993**, 799. (b) Schäfer, A.; Klamt, A.; Sattel, D.; Lohrenz, J. C. W.; Eckert, F. *Phys. Chem. Chem. Phys.* **2000**, *2*, 2187.
(22) Andrae, D.; Häussermann, U.; Dolg, M.; Stoll, H.; Preuss, H. *Theor. Chim. Acta* **1990**, *77*, 123.
(23) Bergner, A.; Dolg, M.; Küchle, W.; Stoll, H.; Preuss, H. *Mol. Phys.* **1993**, *80*, 1431.
(24) Martin, J. M. L.; Sundermann, A. *J. Chem. Phys.* **2001**, *114*, 3408.
(25) (a) Dunning, T. H., Jr. *J. Chem. Phys.* **1989**, *90*, 1007. (b) Kendall, R. A.; Dunning, T. H., Jr.; Harrison, R. J. *J. Chem. Phys.* **1992**, *96*, 6796. (c) Woon, D. E.; Dunning, T. H., Jr. *J. Chem. Phys.* **1993**, *98*, 1358.
(26) Peterson, K. A.; Woon, D. E.; Dunning, T. H., Jr. *J. Chem. Phys.* **1994**, *100*, 7410.
(27) de Jong, G. T.; Sola, M.; Visscher, L.; Bickelhaupt, F. M. *J. Chem. Phys.* **2004**, *121*, 9982.
(28) (a) Reed, A. E.; Curtiss, L. A.; Weinhold, F. *Chem. Rev.* **1988**, *88*, 899. (b) Glendening, E. D.; Reed, A. E.; Carpenter, J. E.; Weinhold, F. *NBO Version 3.1*.
(29) Wiberg, K. B. *Tetrahedron* **1968**, *24*, 1083.
(30) Schaftenaar, G.; Noordik, J. H. *J. Comput.-Aided Mol. Des.* **2000**, *14*, 123.

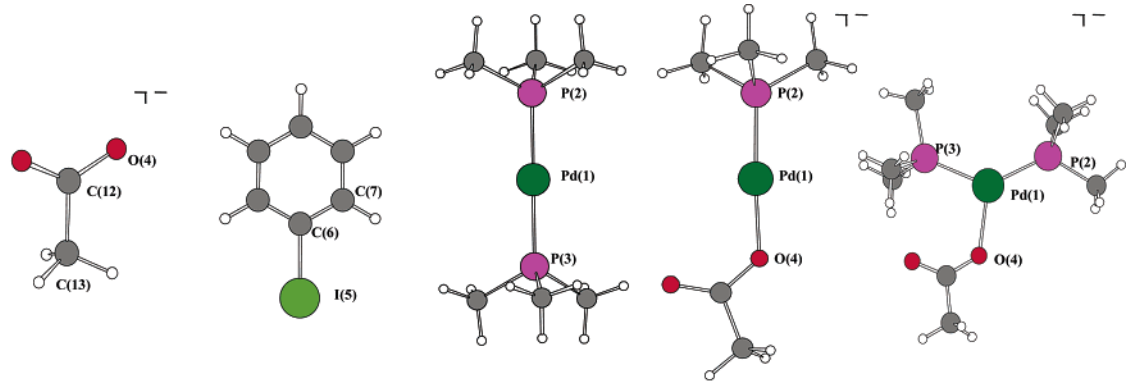

9a	1a	7a	8a
C(12) – O(4) = 1.303	C(6) – I(5) = 2.157	Pd(1) – P(2) = 2.355	Pd(1) – P(2) = 2.253	Pd(1) – P(2) = 2.323
C(12) – C(13) = 1.581	C(6) – C(7) = 1.415	Pd(1) – P(3) = 2.355	Pd(1) – O(4) = 2.100	Pd(1) – P(3) = 2.389
		P – Pd – P = 179.3	P – Pd – O = 177.1	Pd(1) – O(4) = 2.319
				P – Pd – P = 133.2
				P(3) – Pd – O = 103.7
				P(2) – Pd – O = 123.1

Figure 1. Optimized structures of the starting materials (BP86/LANL2DZ), with selected bond lengths (in Å) and angles (in deg).

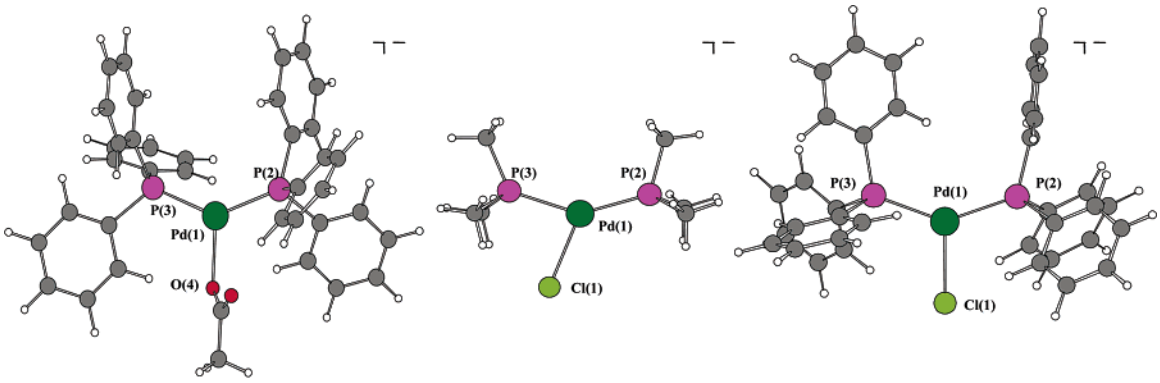

8b	8c	8d
Pd(1) – P(2) = 2.365	Pd(1) – P(2) = 2.315	Pd(1) – P(2) = 2.357
Pd(1) – P(3) = 2.368	Pd(1) – P(3) = 2.399	Pd(1) – P(3) = 2.362
Pd(1) – O(4) = 2.304	Pd(1) – Cl(1) = 2.656	Pd(1) – Cl(1) = 2.601
P – Pd – P = 136.6	P – Pd – P = 144.8	P – Pd – P = 140.0
P(3) – Pd – O = 109.2	P(3) – Pd – Cl = 87.1	P(3) – Pd – Cl = 111.5
P(2) – Pd – O = 113.5	P(2) – Pd – Cl = 128.0	P(2) – Pd – Cl = 108.3

Figure 2. Optimized structures of **8b**, **8c**, and **8d** (BP86/LANL2DZ), with selected bond lengths (in Å) and angles (in deg).

metrical. In a recent B3LYP/LACVP* study,[31] stable structures were identified for **8d** and $Pd(PH_3)_2Cl^-$ (**8e**), but no minimum was found for **8c**. To clarify this discrepancy, we performed further B3LYP/LACVP* calculations.

We confirm the published results[31] for **8d** and **8e**. B3LYP/LACVP* geometry optimization of **8c** leads to dissociation of chloride on starting from an initial symmetric structure similar to **8e** and to a local minimum on starting from the distorted BP86/LANL2DZ structure of **8c**, so that B3LYP/LACVP* and BP86/LANL2DZ are actually consistent with each other. Given the doubts on whether PMe_3 is a suitable model ligand in three-coordinate palladium complexes,[31] we have carried out further calculations on **8a** at the BP86/LACVP*, BP86/EXT, and MP2/LANL2DZ levels which invariably give energy minima with distorted geometries (similar to the BP86/LANL2DZ structure of **8a** shown in Figure 1). Unless noted otherwise, all results in the following sections refer to BP86/LANL2DZ by default.

B. Coordination of Aryl Halides to Palladium(0) Species. After these studies on three-coordinate anionic palladium(0) species, we investigated possible structures for the initial product of the oxidative addition of phenyl iodide **9** to these compounds. We first focused on five-coordinate complexes, as proposed by Amatore and Jutand.[8] However, despite intensive searches starting from compounds **8a**, **8b**, and **8c**, we did not find any energy minima for five-coordinate palladium species

(31) Kozuch, S.; Shaik, S.; Jutand, A.; Amatore, C. *Chem. Eur. J.* **2004**, *10*, 3072.

Table 1. Energetics (kcal/mol) for the Coordination of the Phenyl Halide

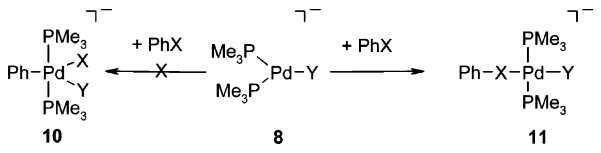

10 8 11

X	Y	ΔE_e	ΔE_0	ΔH_{298}	ΔG_{298}	ΔE_{sov}
I	OAc^-	−20.3	−19.4	−18.6	−9.3	−12.5
Br	OAc^-	−13.6	−12.9	−12.1	−2.5	−6.0
Cl	OAc^-	−5.8	−5.4	−4.5	5.0	1.7
I	Cl^-	−21.9	−21.0	−20.3	−9.2	−15.4

containing both a phenyl and an iodide ligand. For any chosen starting geometry, all investigated palladium species with five ligands immediately lost one of them to form stable four-coordinate complexes.[10] The gradual approach of a phenyl iodide molecule to the three-coordinate species **8a** and slow cleavage of the C−I bond also did not lead to stable structures. In alternative attempts, we started out from a square-planar complex and brought a fifth ligand closer to the metal center. In this case, one of the other ligands dissociated upon the formation of the new bond. Solely by freezing the palladium−ligand bonds or certain bond angles during optimization, we were able to minimize the energies of such constrained five-coordinate structures. However, as soon as the restrictions were removed, one of the ligands dissociated.

To make sure that these failures were not due to gas-phase effects, we also tried to optimize the geometry of selected five-coordinate species in a solvent (THF) using the COSMO methodology as implemented in TURBOMOLE.[21,32] However, these calculations gave analogous results. In view of all these futile attempts, we have serious doubts that such five-coordinate palladium(0) species with monodentate ligands can exist in the gas phase or in solution and that they could be decisive intermediates in catalytic processes.

In the course of these calculations, we discovered that the phenyl iodide molecule is strongly attracted to the anionic palladium species, giving rise to an intermediate with entirely different geometry: almost independent of the orientation of these two fragments, a gradual approach leads to the formation of a four-coordinate square-planar complex (**11a**), in which the phenyl iodide linearly coordinates to the palladium center (Table 1). Geometry optimizations of several precoordination complexes (e.g. van der Waals gas-phase adducts) produce the same energy minimum.

The formation of **11a** is highly exothermic and exergonic ($\Delta E_e = -20.3$ kcal/mol, $\Delta G_{298} = -9.3$ kcal/mol) with respect to the starting materials (**8a** and **9**) and occurs without a significant energy barrier. Therefore, this complex should be formed rapidly under experimental conditions, without giving rise to free acetate or iodide ions. This is fully consistent with the experimental findings by Amatore and Jutand: that almost immediately after addition of phenyl iodide to a solution of an anionic palladium(0) complex both compounds disappear, but neither free acetate nor iodine can be detected.[8]

(32) Ahlrichs, R.; Bär, M.; Häser, M.; Horn, H.; Kölmel, C. *Chem. Phys. Lett.* **1989**, *162*, 165.

Scheme 4. Coordination of Phenyl Iodide to Palladium(0) Species

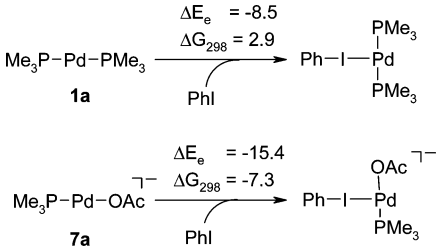

To validate the stability of the intermediate **11a**, we recalculated its structure with a significantly larger basis set (BP86/EXT; see Computational Details) and also found an energy minimum. With **8a**, **9**, and **11a** fully optimized at the BP86/EXT level, the reaction **8a** + **9** → **11a** is predicted to be highly exothermic ($\Delta E_e = -14.5$ kcal/mol). Furthermore, structure **11a** remained stable during a full solvent optimization (THF) using the COSMO methodology (BP86/LANL2DZ). Finally, we confirmed that the coordination of phenyl iodide is more favorable than a possibly competing coordination of donor ligands, such as THF: all attempts to optimize the geometry of an adduct between **8a** and a single THF molecule resulted in the dissociation of this additional ligand from the metal center. Therefore, the direct formation of **11a** is likely to occur also under experimental conditions in a polar solvent such as THF.

The formation of such a four-coordinate adduct is also possible when starting from the anionic palladium species **8c** containing a chloride instead of an acetate ligand ($\Delta E_e = -21.9$ kcal/mol, $\Delta G_{298} = -9.2$ kcal/mol). The coordination of a phenyl iodide molecule to the coordinatively unsaturated anionic monophosphine complex $Pd(PMe_3)OAc^-$ is also quite exergonic ($\Delta G_{298} = -7.3$ kcal/mol). In contrast to this, the coordination of phenyl iodide to the neutral complex $Pd(PMe_3)_2$ (**1a**), yielding a T-shaped structure, is much less favorable ($\Delta G_{298} = 2.9$ kcal/mol) (Scheme 4). These differences may help to explain the different performance of catalysts generated in situ from different palladium(II) or palladium(0) precursors.

It is particularly interesting to investigate whether structures of the general formula **11** are also stable for phenyl bromide or phenyl chloride, since these halides are widely used in catalytic processes. The formation of a four-coordinate species of type **11** is possible for phenyl bromide ($\Delta E_e = -13.6$ kcal/mol, $\Delta G_{298} = -2.6$ kcal/mol), while the formation of an adduct between **8a** and phenyl chloride is still exothermic but no longer exergonic ($\Delta E_e = -5.8$ kcal/mol, $\Delta G_{298} = 5.0$ kcal/mol). This agrees with the experimental finding that catalytic reactions involving aryl chloride require special conditions, i.e., the use of sterically highly demanding electron-rich ligands. Under these conditions, alternative reaction pathways via coordinatively unsaturated anionic palladium species similar to **7a** might become prevailing.[6]

The palladium(0) intermediates **11a**−**d** are almost square-planar complexes with linearly bound aryl halides. They can be best seen as "ate" complexes of iodine,[18] since upon complexation of phenyl iodide to the $Pd(PMe_3)_2OAc^-$ fragment **8a**, the electron density at the phenyl iodide is increased by 0.505e (0.249e at I), mainly

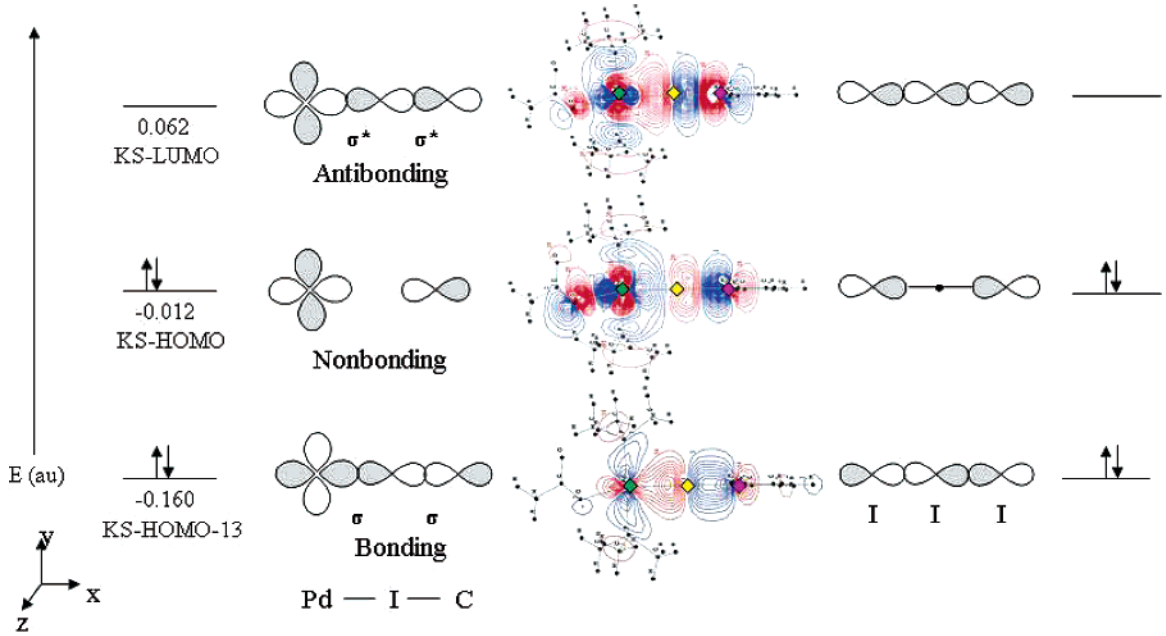

Figure 3. Contour maps of some important KS-MOs for intermediate **11a** (BP86/LANL2DZ). Given on the left are Kohn–Sham orbital energies (in au). Contour values are 0.00, ±0.007, ±0.014, ±0.021, ±0.028, ... (in $e^{1/2}$ $au^{-3/2}$). Blue and red lines represent positive and negative values, respectively. Pd(1), I(5), and C(6) are marked by green, yellow, and pink diamonds, respectively. Schematic orbital diagrams are included for the I_3^- anion.

due to a charge transfer from the Pd metal into the antibonding σ^*(C–I) orbital. During this complexation, the C–I bond is elongated by as much as 0.279 Å (13%) and the length of the palladium–acetate bond is increased from 2.319 Å in **8a** to 2.436 Å (5%) in **11a**. Only slight changes are observed for the Pd–P bonds, while the P–Pd–P bond angle increases from 133.2° to 174.2°.

The bonding situation within the linear "Pd(1)–I(5)–C(6)" framework in **11a** is somewhat analogous to that in the hypervalent linear species I_3^-.[33] In accordance with the σ interactions in an I_3^- ion, we observe in KS-HOMO-13, KS-HOMO, and KS-LUMO a bonding, a nonbonding and an antibonding interaction, respectively, along the Pd–I–C framework (Figure 3) where "HOMO-*n*" represents the *n*th occupied orbital below KS-HOMO. The antibonding palladium–acetate interaction in KS-HOMO (involving $d_{x^2-y^2}$ at Pd and p_x at O(4)) becomes more pronounced in the course of the rearrangement **11a** → **12a** with the dissociation of acetate. In the Supporting Information, the electronic structure of **11a** is further characterized by an analysis of the electron density.[34]

C. Mechanism of Oxidative Addition to Anionic Palladium(0) Species. While the formation of **11a** from phenyl iodide and the anionic palladium(0) complex **8a** should proceed very rapidly, the actual oxidative addition reaction can be expected to be a rather complicated process, since the phenyl iodide has to turn around before a cleavage of the C–I bond can be initiated.

According to our calculations this rearrangement is a multistep process leading to the π complex **14a**, which is the starting point of the actual C–X cleavage step (Table 2). The energetics of this sequence is summarized in Table 2. It is evident that, in contrast to the initial coordination of the phenyl iodide, this process requires significant activation energy. The calculated geometries of the intermediates and transition states and some of their important structural features are shown in Figure 4.

Table 2. Energetics (kcal/mol) for the Reaction Pathway from 11a to 14a

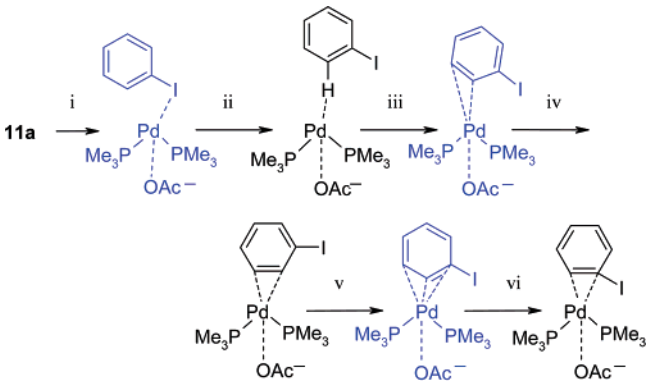

	reacn step					
	i	ii	iii	iv	v	vi
ΔE_e	12.6	−1.8	2.2	−10.3	6.7	−9.9
ΔE_0	12.5	−1.6	1.8	−9.8	6.3	−9.2
ΔH_{298}	11.5	−0.8	1.3	−9.8	6.0	−8.9
ΔG_{298}	15.1	−4.2	2.4	−6.8	6.9	−9.9
ΔE_{sov}	9.2	−0.7	2.3	−9.7	6.9	−9.8
ΔE_{EXT}	9.7	−0.5	1.9	−9.3	7.6	−9.5

Starting from intermediate **11a**, a linear transit search shortening the C(6)–Pd(1) distance led to the discovery of intermediate **12a**. One of the characteristic features of **12a** is the presence of a C–H interaction with palladium, while both of the Pd–P distances are almost equivalent (Figure 4). Reaching the correspond-

(33) Shriver, D. F.; Atkins, P. W.; Langford, C. H. *Inorganic Chemistry,* 2nd ed.; Oxford University Press: Oxford, U.K., 1994.

(34) (a) Bader, R. F. W. *Chem. Rev.* **1991**, *91*, 893. (b) Bader, R. F. W.; Popelier, P. L. A.; Keith, T. A. *Angew. Chem., Int. Ed. Engl.* **1994**, *33*, 620. (c) Bader, R. F. W.; Matta, C. F. *Inorg. Chem.* **2001**, *40*, 5603. (d) Bader, R. F. W.; Matta, C. F.; Cortés-Guzmán, F. *Organometallics* **2004**, *23*, 6253.

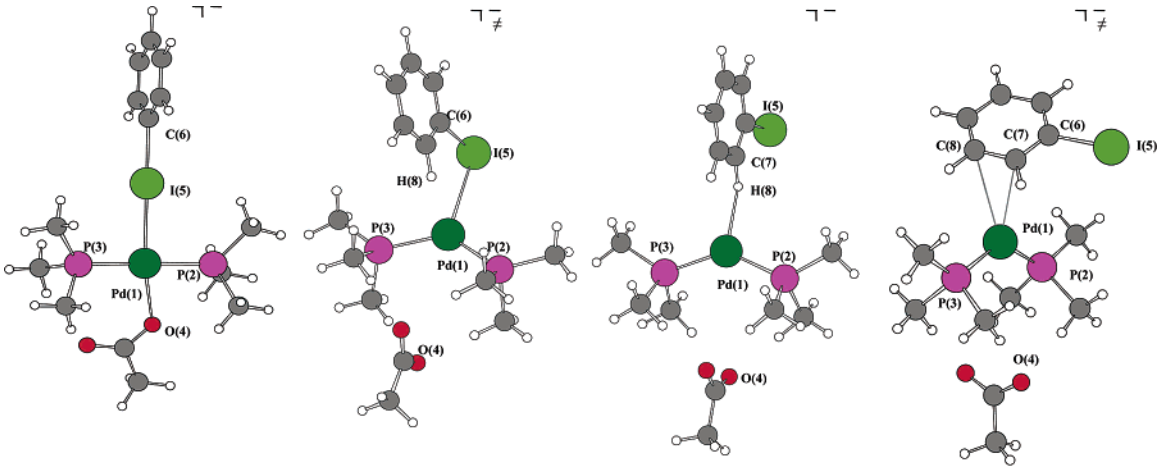

Pd(1) – P(2) = 2.389
Pd(1) – P(3) = 2.384
Pd(1) – O(4) = 2.436
Pd(1) – I(5) = 2.949
Pd(1) – C(6) = 5.344
I(5) – C(6) = 2.401
P – Pd – P = 174.2
C(6) – I – Pd = 174.6
P(3) – Pd – O = 102.3

11a

Pd(1) – P(2) = 2.375
Pd(1) – P(3) = 2.371
Pd(1) – O(4) = 4.627
Pd(1) – I(5) = 3.329
Pd(1) – C(6) = 3.852
I(5) – C(6) = 2.162
Pd(1) – H(8) = 2.318
P – Pd – P = 128.9
C(6) – I – Pd = 86.3

[11a-12a]$^{\neq}$

Pd(1) – P(2) = 2.361
Pd(1) – P(3) = 2.360
Pd(1) – O(4) = 4.381
Pd(1) – I(5) = 5.357
Pd(1) – C(6) = 4.566
I(5) – C(6) = 2.175
Pd(1) – H(8) = 2.348
Pd(1) – C(7) = 3.286
Pd(1) – C(8) = 3.596
P – Pd – P = 138.2

12a

Pd(1) – P(2) = 2.382
Pd(1) – P(3) = 2.378
Pd(1) – O(4) = 4.585
Pd(1) – I(5) = 4.765
Pd(1) – C(6) = 3.788
I(5) – C(6) = 2.168
Pd(1) – C(7) = 2.756
Pd(1) – C(8) = 3.075
P – Pd – P = 130.3

[12a-13a]$^{\neq}$

Pd(1) – P(2) = 2.460
Pd(1) – P(3) = 2.467
Pd(1) – O(4) = 5.165
Pd(1) – I(5) = 4.683
Pd(1) – C(6) = 3.153
I(5) – C(6) = 2.186
Pd(1) – C(7) = 2.220
Pd(1) – C(8) = 2.191
P – Pd – P = 103.5

13a

Pd(1) – P(2) = 2.461
Pd(1) – P(3) = 2.451
Pd(1) – O(4) = 5.148
Pd(1) – I(5) = 3.884
Pd(1) – C(6) = 2.603
I(5) – C(6) = 2.179
Pd(1) – C(7) = 2.161
Pd(1) – C(8) = 2.591
P – Pd – P = 108.1

[13a-14a]$^{\neq}$

Pd(1) – P(2) = 2.454
Pd(1) – P(3) = 2.467
Pd(1) – O(4) = 5.182
Pd(1) – I(5) = 3.639
Pd(1) – C(6) = 2.089
I(5) – C(6) = 2.337
Pd(1) – C(6) = 2.089
Pd(1) – C(7) = 2.245
P – Pd – P = 102.6

14a

Figure 4. Optimized structures of intermediates **11a**−**14a**, with selected bond lengths (in Å) and angles (in deg).

ing transition state **[11a-12a]**‡ requires only a moderate activation of 12.6 kcal/mol (ΔE_e), and this is already the highest energy barrier in the whole process of the oxidative addition. The imaginary frequency at the transition state reflects the incoming motion of H(8) toward Pd(1) and simultaneous removal of I(5). The flatness of the potential energy surface in this region is manifested in the low imaginary frequency of **[11a-12a]**‡ ($25i$ cm^{-1}).

Concurrent with the approach of the phenyl iodide, an early dissociation of the acetate is observed; in **[11a-12a]**‡ the Pd−O(4) distance already amounts to 4.627 Å. A weak bonding interaction of both H(8) and I(5) with palladium can be considered, similar to that observed by Bickelhaupt et al. for methyl chloride complexes.[9] The interaction of H(8) with the metal center in **[11a-12a]**‡ is manifested in an elongated C(7)−H(8) bond distance (1.115 Å). According to the second-order per-

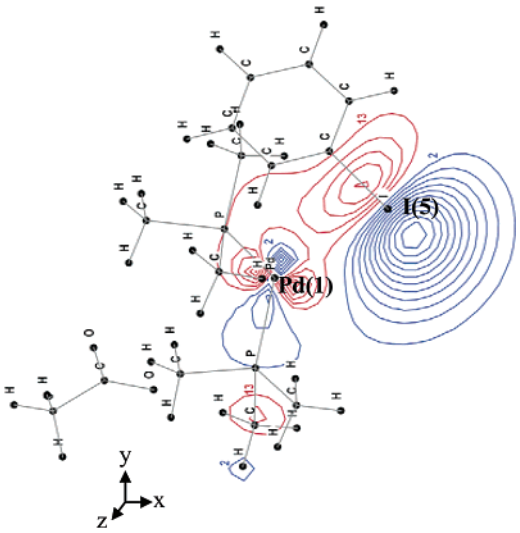

Figure 5. KS-LUMO for **[11a-12a]**‡. Contour values are 0.00, ±0.007, ±0.014, ±0.021, ±0.028, ... (in $e^{1/2}$ $au^{-3/2}$). Blue and red lines represent negative and positive values, respectively.

turbational NBO analysis, there is a weak donor−acceptor interaction between a d orbital of the palladium and the σ^*(C(7)−H(8)) bond orbital (accounting for ∼4 kcal/mol). Figure 5 shows the KS-LUMO for **[11a-12a]**‡, in which a bonding orbital interaction between Pd(1), H(8) and C(5)−I(6) is visible.

In comparison to **[11a-12a]**‡, the intermediate **12a** is only 1.8 kcal/mol (ΔE_e) lower in energy. The rearrangement from **12a** to **13a** through the transition state **[12a-13a]**‡ requires an activation energy of only 2.2 kcal/mol (ΔE_e). The mode corresponding to the single imaginary frequency of **[12a-13a]**‡ indicates a wagging motion of the phenyl iodide moiety toward the metal center.

π complexes of type **13a** with η^2 bonding of palladium to the C(7)−C(8) π bond have been discussed for various organometallic reactions.[9−11,19] The NBO analysis of **13a** reveals an electron donation from the π(C(7)−C(8)) bond orbital to the metal s orbital, along with a back-donation from the d_π orbital of the metal to the π^*(C(7)−C(8)) bond orbital. The presence of the electron-rich trimethylphosphine ligands increases the electron density on the metal center, and thus enhances the electron donating ability. In the η^2 palladium(0) π complex **13a**, both the C(8)−Pd(1) and C(7)−Pd(1) bond distances are much shorter than in the transition state **[12a-13a]**‡ (Figure 4), and the P−Pd−P bond angle decreases by 26.7°, concomitant with an increase in the Pd−acetate distance by almost 0.6 Å. Obviously, the P−Pd−P angle is very sensitive to the position of the acetate: moving the acetate out of the coordination zone of palladium allows for smaller angles.

From intermediate **13a**, the reaction continues via a transition state (**[13a-14a]**‡) to another π complex, **14a**. This complex is more stable than **13a** and is an ideal precursor for the C−I cleavage reaction. The transition state **[13a-14a]**‡ has an activation energy of 6.7 kcal/mol (ΔE_e) and is characterized by a single imaginary frequency (68.3*i* cm^{-1}). The imaginary mode describes the simultaneous breaking of the C(8)−Pd(1) bond and the formation of the C(6)−Pd(1) bond. There is a considerable increase in the C(8)−Pd(1) distance (by 0.400 Å) in **[13a-14a]**‡ as compared to **13a**, while both

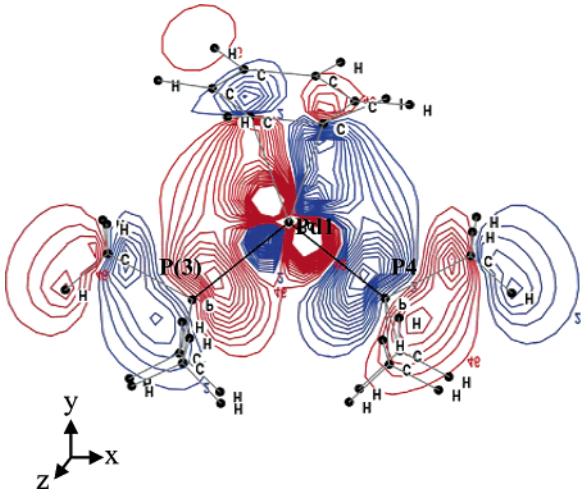

Figure 6. Kohn−Sham HOMO-2 orbital of **14a**. Contour values are 0.00, ±0.007, ±0.014, ±0.021, ±0.028, ... (in $e^{1/2}$ $au^{-3/2}$). Blue and red lines represent negative and positive values, respectively.

the C(6)−Pd(1) and C(7)−Pd(1) distances are shortened (by 0.550 and 0.059 Å).

A closer look at the η^3 transition state (**[13a-14a]**‡) reveals a perpendicular orientation of the C(8)−C(7)−C(6) plane with respect to the P−Pd−P plane. The elongated C(7)−C(8) and C(7)−C(6) distances (1.457 and 1.451 Å) in the phenyl group reflect the loss of double-bond character in this three-center bond. Interestingly, both in **13a** and **14a**, the η^2 bonding axis is coplanar with the P−Pd−P plane. Hence, during the reaction the square-planar geometry of the reactant (**13a**) changes to a quasi-tetrahedral transition state (**[13a-14a]**‡) and then back to the square-planar product (**14a**). Recently, a similar type of "ring-hopping" transition state has been discussed by Reinhold et al. while studying the C−F bond activation in $M(H_2PCH_2CH_2PH_2)(C_6F_6)$ (M = Ni, Pt) complexes.[35]

The product **14a** is stabilized by bonding and back-bonding interactions between palladium and the C(6)−C(7) moiety. The latter are clearly visible in KS-HOMO-2 (see Figure 6), involving d_{xy} at palladium and π^* at C(6)−C(7).

D. Cleavage of the Carbon−Iodine Bond: Path A. We have identified two possible pathways for the cleavage of the C−I bond in **14a**, leading to two different species (**15a** and **18a**). In both of them, the phosphines are located cis to each other. We could not identify a pathway leading directly to the more stable trans compound **3a**. This is consistent with experimental findings by Espinet et al. They added $C_6Cl_2F_3I$ to $Pd(PPh_3)_4$ at room temperature and observed that, initially, *cis*-$[Pd(C_6Cl_2F_3)I(PPh_3)_2]$ was formed, which upon heating rearranged to the trans isomer.[7]

In **14a**, the acetate is held by long-range electrostatic interactions in the complex. When we decreased the palladium−acetate distance, the C(6)−I(5) distance started to increase and, finally, the C−I bond broke and the iodide dissociated, giving rise to the palladium(II) complex **15a**. The transition state (**[14a-15a]**‡) has an activation barrier of only 8.5 kcal/mol (ΔE_e; Table 3).

(35) Reinhold, M.; McGrady, J. E.; Perutz, R. N. *J. Am. Chem. Soc.* **2004**, *126*, 5268.

Table 3. Energetics (kcal/mol) for the Cleavage of the Carbon−Iodine Bond with Removal of the Iodide (Path A)

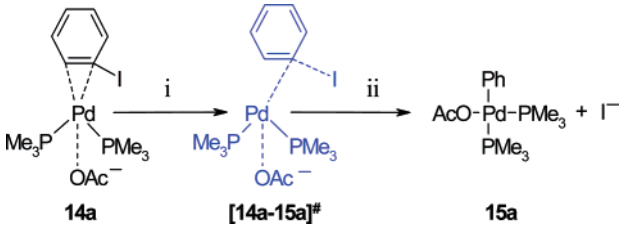

	reacn step	
	i	ii
ΔE_e	8.5	−20.9
ΔE_0	8.2	−19.0
ΔH_{298}	7.9	−18.7
ΔG_{298}	10.3	−27.7
ΔE_{sov}	6.8	−42.5
ΔE_{EXT}	10.6	−16.6

As one goes from **14a** to [**14a-15a**]‡, the coordination of the phenyl ring changes from η^2 to η^1, and the acetate coordinates to the newly available position. In the transition state, the Pd(1)−O(4) and C(6)−I(5) distances amount to 2.645 and 2.799 Å, respectively, and the C(6)−I(5) bond becomes highly polarized: The NPA charge on I(5) is increased from −0.074e in **14a** to −0.464e in [**14a-15a**]‡ (reflecting the formation of an iodide anion). The imaginary mode of 47.6*i* cm^{-1} in [**14a-15a**]‡ represents the simultaneous addition of acetate and removal of I(5) from Pd(1).

In the presence of a polar solvent, the generation of solvated iodide will be more facile than in the gas phase. Indeed, COSMO calculations performed in a solvent field (THF) reduce the energy difference between **14a** and [**14a-15a**]‡ to 6.8 kcal/mol (ΔE_{sov}) and increase the subsequent energy release to −42.5 kcal/mol (ΔE_{sov}).

The final product **15a** (Figure 7) of the oxidative addition is a neutral, square-planar d^8 palladium(II) complex. The P−Pd−P angle is 101.6°, and the Pd(1)−P(2) distance is greater than the Pd(1)−P(3) distance,

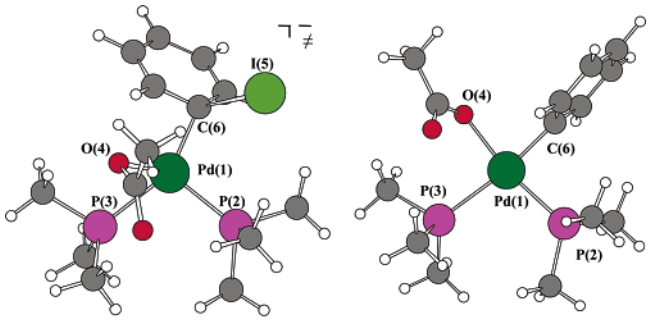

Pd(1) – P(2) = 2.401
Pd(1) – P(3) = 2.481
Pd(1) – O(4) = 2.645
Pd(1) – I(5) = 3.960
Pd(1) – C(6) = 2.023
I(5) – C(6) = 2.799
P – Pd – P = 104.0
I – C(6) – Pd = 109.4

Pd(1) – P(2) = 2.363
Pd(1) – P(3) = 2.495
Pd(1) – O(4) = 2.110
Pd(1) – C(6) = 2.040
P – Pd – P = 101.6

[14a-15a]‡ **15a**

Figure 7. Optimized structures of [**14a-15a**]‡ and **15a**, with selected bond lengths (in Å) and angles (in deg).

Table 4. Energetics (kcal/mol) for the Reaction Pathway from 14a to 18a (Path B)

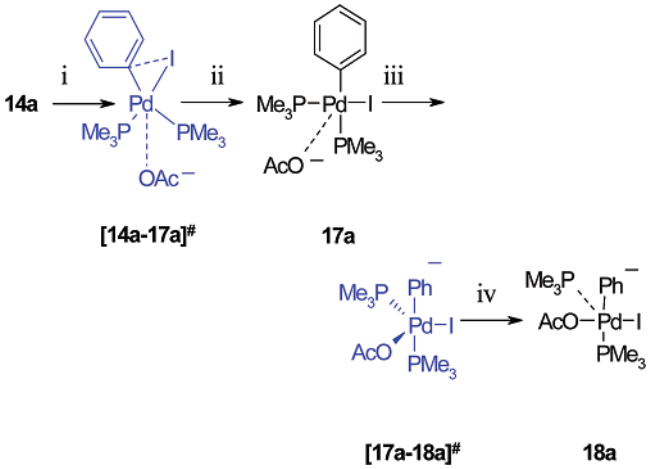

	reacn step			
	i	ii	iii	iv
ΔE_e	2.6	−34.7	12.7	−7.6
ΔE_0	2.7	−33.1	11.1	−7.2
ΔH_{298}	2.3	−33.0	11.3	−6.6
ΔG_{298}	3.2	−32.4	11.4	−9.9
ΔE_{sov}	2.1	−34.9	13.5	−6.5
ΔE_{EXT}	4.7	−35.2	17.3	−5.2

due to the strong trans influence of the phenyl group. During the reactions discussed in sections C and D, the acetate is close to the metal in **11a**, [**14a-15a**]‡, and **15a**. In all other species, it is a remote ligand, which remains in proximity to the hydrogen atoms of a PMe_3 group. In solution, one may expect that these weak gas-phase interactions will not survive and that acetate will be solvated.[19]

E. Cleavage of the Carbon−Iodine Bond: Path B. Looking for an alternative C−I cleavage, we performed a linear transit scan decreasing the Pd(1)−I(5) distance in **14a**. In this case, the iodine remained bound to the palladium, while the acetate was liberated giving rise to complex **17a**. Since the transition state [**14a-17a**]‡ has a slightly lower energy (ΔE_e = 2.6 kcal/mol, ΔG_{298} = 3.2 kcal/mol; Table 4) in comparison to [**14a-15a**]‡, this pathway might be kinetically favored. As one goes from **14a** to [**14a-17a**]‡, the C(6)−I(5) distance increases by 0.35 Å, while the Pd(1)−I(5) distance decreases by an amount of 0.23 Å. In [**14a-17a**]‡ the iodine atom is oriented such that the C(6)−I(5) axis is almost perpendicular to the P−Pd−P plane, with the C(6)−C(7) η^2 coordination diminishing as iodine approaches.

Several groups performed similar calculations on H−H and C−H σ-bond activation reactions of metal phosphine complexes $M(PH_3)_2$ (M = Pd, Pt)[36,37] and found that the oxidative addition proceeds through an approach of the substrate parallel to the P−Pd−P plane. This appears reasonable, since the electron back-donation to the σ^* orbital, which promotes bond breaking,

(36) (a) Low, J. J.; Goddard, W. A., III. *J. Am. Chem. Soc.* **1984**, *106*, 6928. (b) Obara, S.; Kituara, K.; Morokuma, K. *J. Am. Chem. Soc.* **1984**, *106*, 7482.

(37) (a) Low, J. J.; Goddard, W. A., III. *J. Am. Chem. Soc.* **1984**, *106*, 8321. (b) Low, J. J.; Goddard, W. A., III. *Organometallics* **1996**, *5*, 609. (c) Low, J. J.; Goddard, W. A., III. *J. Am. Chem. Soc.* **1986**, *108*, 6115.

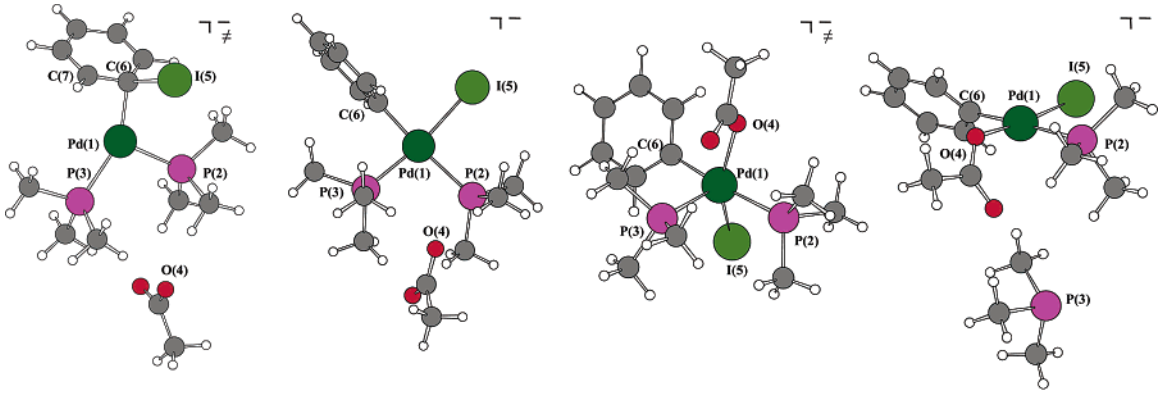

Figure 8. Optimized structures of complexes **[14a-17a]**‡, **17a**, **[17a-18a]**‡, and **18a**, with selected bond lengths (in Å) and angles (in deg).

occurs from the d_π orbital in the P−Pd−P plane and is thus facilitated by electron-donating phosphine ligands. However, other types of transition states for σ-bond activation have also been reported. Sakaki et al. found a largely twisted transition state for the activation of C−C and C−Si σ bonds on the $Pt(PH_3)_2$ complex.[38] Recently, Matsubara et al. explained the activation of the C−Sn σ bond of $HC{\equiv}CSnH_3$ on the $Pd(PH_3)_2$ complex, through a nonplanar, perpendicular approach.[39] Senn et al. described a transition state similar to [**14a-17a**]‡, where the orientation of the ligands around the palladium center is quasi-tetrahedral.[11]

Formation of **17a** from [**14a-17a**]‡ is highly exothermic by −34.7 kcal/mol (ΔE_e). Complex **17a** shows the usual square-planar environment around the metal center with P−Pd−P and I−Pd−C(6) bond angles of 97.3 and 85.5°, respectively. The trans influence of the phenyl group is also prominent in **17a** and leads to a longer P(2)−Pd(1) distance. After direct coordination of I(5) to Pd(1), the NPA charge on the metal center is decreased by 0.032e.

Bringing the acetate closer to palladium in a linear transit scan results in the dissociation of one of the phosphines via a five-coordinated transition state ([**17a-18a**]‡) with acetate and I(5) lying in the equatorial position. The dissociation of iodine might be thermodynamically favorable in solution, but in the gas phase it is endergonic. We observe that the gradual incoming of the acetate from **17a** affords a new intermediate **18a** via the transition state [**17a-18a**]‡. The gas-phase activation barrier is 12.7 kcal/mol (ΔE_e), which slightly increases to 13.5 kcal/mol (ΔE_{sov}) in THF.

In [**17a-18a**]‡, the Pd(1)−P(3) distance is very large (2.732 Å), indicating that the dissociation of the phosphine is quite advanced. The product **18a** is a usual, square-planar palladium(II) complex, with a relatively long Pd(1)−P(2) bond (i.e. 2.488 Å), due to the trans influence of the phenyl group. The second PMe_3 group is completely dissociated and is 5.772 Å away from palladium.

Table 5. Energetics (kcal/mol) for Cis−Trans Isomerization

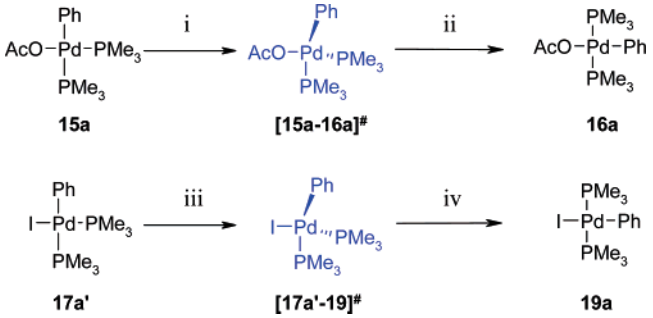

	reacn step			
	i	ii	iii	iv
ΔE_e	21.4	−32.5	19.5	−28.8
ΔE_0	20.4	-31.3	18.4	−27.2
ΔH_{298}	20.4	-31.3	18.5	−27.4
ΔG_{298}	20.2	−31.5	17.9	−26.0
ΔE_{sov}	23.7	−31.9	20.2	−27.2
ΔE_{EXT}	24.3	−33.3	22.4	−32.0

F. Cis−Trans Isomerization. Three different mechanisms are usually considered for a cis−trans isomerization in square-planar complexes: the associative pathway,[40] the Berry pseudorotation mechanism,[41] and the dissociative pathway.[42] Which of them is most favorable depends on the nature of the solvent, the

(38) Sakaki, S.; Mizoe, N.; Musashi, Y.; Biswas, B.; Sugimoto, M. *J. Phys. Chem. A* **1998**, *102*, 8027.
(39) (a) Matsubara, T. *Organometallics* **2003**, *22*, 4286. (b) Matsubara, T.; Hirao, K. *Organometallics* **2002**, *21*, 2662.
(40) Basolo, F.; Pearson, G. *Mechanism of Inorganic Reactions,* 2nd ed.; Wiley: New York, 1967.
(41) (a) Anderson, G. K.; Cross, R. J. *J. Chem. Soc. Rev.* **1980**, *9*, 185. (b) Berry, R. S. *J. Chem. Phys.* **1960**, *32*, 933.
(42) (a) Ozawa, F.; Ito, T.; Nakamura, Y.; Yamamoto, A. *Bull. Chem. Soc. Jpn.* **1981**, *54*, 1868. (b) Pavonessa, R. S.; Trogler, W. C. *J. Am. Chem. Soc.* **1982**, *104*, 3529.

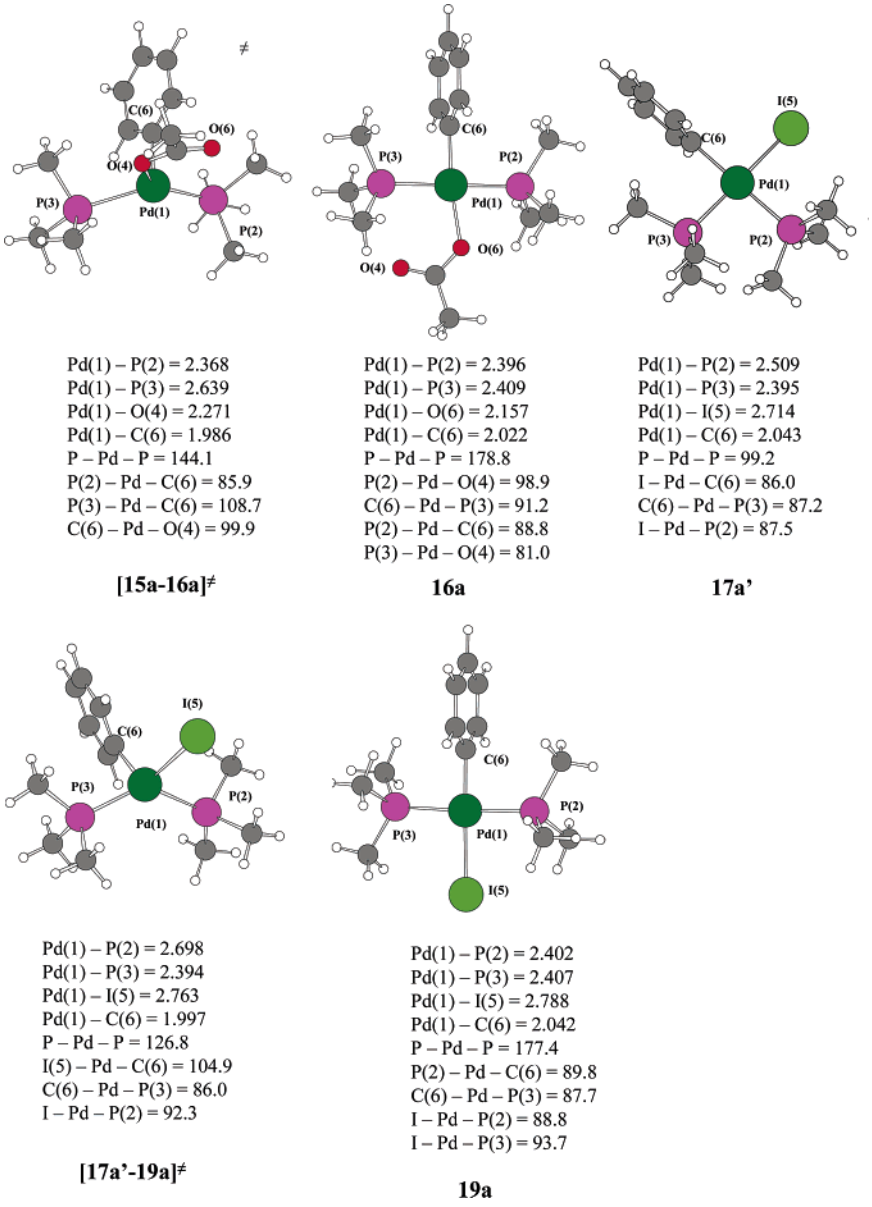

Figure 9. Optimized structures for complexes **[15a-16a]**‡, **16a**, **17a′**, **[17a′-19a]**‡, and **19a**, with selected bond distances (in Å) and angles (in deg).

electronic effects of the ligands, and the temperature. Recently, Casado et al. performed elaborate kinetic studies on the cis−trans isomerization of $PdRX(PPh_3)_2$ (R = aryl, X = halide). They proposed two phosphine (i.e. PPh_3)-dependent and two phosphine-independent associative pathways. On the basis of their kinetic measurements they rule out dissociative pathways via three-coordinate intermediates.[7]

We have calculated a single-step mechanism for the transformation of cis complex **17a′** (i.e. **17a** without the loosely attached OAc^-) to its trans counterpart (**19a**). In solution, the acetate, which is electrostatically attached to the metal complex in **17a** (Figure 8), is expected to be solvated, thereby facilitating its dissociation to form **17a′** (**17a** → **17a′** + OAc^-; ΔE_e = 32.3 kcal/mol, ΔG_{298} = 17.1 kcal/mol, and ΔE_{sov} = 1.7 kcal/mol), and therefore **17a′** may serve as a simple model for the situation in solution.

The cis−trans isomerization is displayed in Table 5. The activation barrier in the gas phase is 19.5 kcal/mol (ΔE_e). The structural parameters for the transition state (**[17a′-19a]**‡) indicate a quasi-tetrahedral species, arising from an intramolecular rearrangement, which can be viewed as a rotation of the C(6)−Pd−I moiety relative to P−Pd−P with concomitant opening of the respective angles. The Pd(1)−C(6) bond length of 1.997 Å in **[17a′-19a]**‡ is shorter than the values found for **17a′** (2.043 Å) and **19a** (2.042 Å), respectively. The P(2)−Pd(1) bond is longer (2.509 Å) than the P(3)−Pd(1) bond (2.394 Å), due to the higher trans effect of the phenyl group in **17a′**. For the same reason, the Pd(1)−I(5) bond is longer (2.788 Å) in **19a** than in **17a′**. We also studied a similar cis−trans isomerization reaction starting from the cis complex **15a**. The latter eventually connects (Figure 9) to a quasi-tetrahedral transition state (**[15a-16a]**‡), which then affords the trans complex **16a**. The activation barrier for isomerization of **15a** to **16a** is 21.4 kcal/mol (ΔE_e) and thus is only about 2 kcal/mol higher than that for the isomerization of **17a′** to **19a** (Table 5). Quasi-tetrahedral d^8 transition-metal species tend to

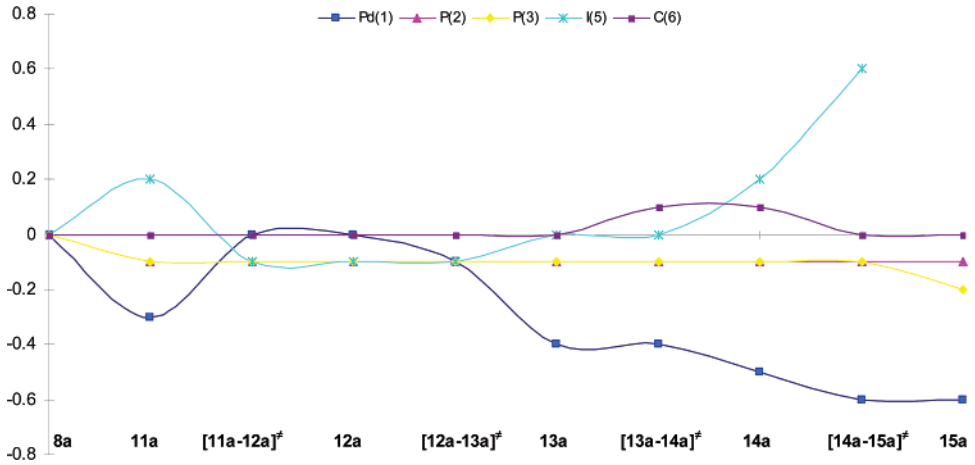

Figure 10. Natural population changes of selected atoms during Pd−I oxidative addition to **8a**. Positive and negative signs represent decreases and increases in population, respectively, relative to **8a**.

have low-lying triplet states, and we have therefore checked their energies in the transition states **[15a-16a]**‡ and **[17a′-19a]**‡. In both cases, the lowest triplet lies significantly higher than the lowest singlet in single-point calculations at the singlet geometry, and reoptimization of the transition states on the triplet surface puts them 16.6 and 15.3 kcal/mol, respectively, above their singlet counterparts. Hence, triplet pathways are apparently not competitive in the intramolecular cis−trans isomerizations studied presently, while they may play an essential role in other systems.[35]

We have made some attempts to locate five-coordinate transition states for an associative mechanism, but without success, which might not be too surprising in view of our failure to find the postulated five-coordinate intermediates of the Amatore−Jutand mechanism (see section B). Five-coordinate transition states for cis−trans isomerizations have been reported in the literature for other related systems: e.g., in the case of square-planar $PtH(SiH_3)(PH_3)_2$, where a PH_3-promoted cis−trans isomerization via a Berry pseudorotation mechanism requires an activation energy of 28 kcal/mol at the MP4SDQ level.[43,44] We cannot exclude the existence of such pathways in our system with certainty, but it would seem unlikely for them to be more facile than the studied intramolecular cis−trans isomerizations with calculated barriers of ca. 20 kcal/mol (see Table 5).

G. Charge Distributions. Figure 10 illustrates the atomic population of the key atoms involved in the oxidative addition process, while selected NPA charges and Wiberg bond indices for various complexes and intermediates are listed in the Supporting Information. The lowering of palladium d orbital population during the reaction is consistent with the process of oxidative addition. The significant increase of I(5) population in **11a**, with the concomitant lowering of the palladium population, reflects the charge transfer from palladium to the I(5)−C(6) bond. In the species after **11a**, the I(5) population decreases again, because there is no direct coordination to the metal center and, hence, no charge transfer. The rise of the I(5) population from **14a** onward is due to the generation of an iodide anion by dissociation.

Conclusions

In this work we have explored several reaction pathways for oxidative addition reactions of aryl halides to palladium(0) species. Our results confirm that three-coordinate anionic palladium(0) species as proposed by Amatore and Jutand should be stable and can indeed serve as starting points for catalytic reactions. However, we did not find any evidence for the existence of the proposed five-coordinate palladium(II) complexes. Instead, stable four-coordinate intermediates were found, in which the aryl halides coordinate linearly to the palladium via the halide atom. There is no significant energy barrier for the formation of these species, which is consistent with the experimental findings that within seconds after the addition of iodobenzene to a Pd catalyst, neither the initial palladium(0) species nor free iodide or acetate is detectable.

Furthermore, we have identified two energetically feasible reaction pathways for the actual C−X cleavage reaction starting from these adducts, confirming that such hypervalent halide species may indeed be the initial intermediates formed in catalytic reactions. In the more favorable one, the acetate counterion initially bound to the palladium catalyst remains at the catalytic center, while the halide originating from the substrate is liberated. Both reaction pathways lead to the formation of cis-configured palladium(II) complexes. Since a subsequent cis−trans isomerization of these complexes to the isolable trans complexes requires significant activation energy, we consider catalytic cycles consisting solely of cis-configured intermediates to be favorable in palladium chemistry.

In conclusion, some fundamental steps of palladium catalyzed cross-coupling reactions have been elucidated. In our ongoing work, we are focusing on further catalytic steps such as transmetalation and reductive elimination.

(43) Sakaki, S.; Mizoe, N.; Musashi, Y.; Sugimoto, M. *J. Mol. Struct. (THEOCHEM)* **1999**, *461−462*, 533.
(44) Sakaki, S.; Mizoe, N.; Sugimoto, M.; Musashi, Y. *Coord. Chem. Rev.* **1999**, *190−192*, 933.

Acknowledgment. We are grateful to the DFG and the BMBF for financial support. L.J.G. thanks Prof. Dr. M. T. Reetz for his constant encouragement and generous support. D.K. thanks Dr. M. Bühl, Dr. K. Angermund, Dr. H. M. Senn, Dr. S. Vyboishchikov, and H. U. Wüstefeld for fruitful and stimulating discussions.

Supporting Information Available: Listings giving gas-phase energies and Cartesian coordinates of all DFT optimized structures, analysis of the electron density in **11a**, selected NPA charges, and Wiberg bond indices in **8a**−**19a**.

OM0500220